Molecules and Cells

FADD Phosphorylation Modulates Blood Glucose Levels by Decreasing the Expression of Insulin-Degrading Enzyme

Yan Lin[1,2], Jia Liu[1], Jia Chen[1], Chun Yao[1], Yunwen Yang[1], Jie Wang[1], Hongqin Zhuang[1,*], and Zi-Chun Hua[1,3,4,*]

[1]The State Key Laboratory of Pharmaceutical Biotechnology, School of Life Sciences, Nanjing University, Nanjing 210023, China, [2]School of Nursing, Xinxiang Medical University, Xinxiang 453000, China, [3]Changzhou High-Tech Research Institute of Nanjing University and Jiangsu TargetPharma Laboratories Inc., Changzhou 213164, China, [4]Shenzhen Research Institute of Nanjing University, Shenzhen 518057, China
*Correspondence: hzc1117@nju.edu.cn (ZCH); hqzhuang@nju.edu.cn (HZ)
https://doi.org/10.14348/molcells.2020.2198
www.molcells.org

Our previous study revealed a novel role of Fas-associated death domain-containing protein (FADD) in islet development and insulin secretion. Insulin-degrading enzyme (IDE) is a zinc metalloprotease that selectively degrades biologically important substrates associated with type 2 diabetes (T2DM). The current study was designed to investigate the effect of FADD phosphorylation on IDE. We found that the mRNA and protein levels of IDE were significantly downregulated in FADD-D mouse livers compared with control mice. Quantitative real-time polymerase chain reaction analysis showed that FADD regulates the expression of IDE at the transcriptional level without affecting the stability of the mRNA in HepG2 cells. Following treatment with cycloheximide, the IDE protein degradation rate was found to be increased in both FADD-D primary hepatocytes and FADD-knockdown HepG2 cells. Additionally, IDE expression levels were reduced in insulin-stimulated primary hepatocytes from FADD-D mice compared to those from control mice. Moreover, FADD phosphorylation promotes nuclear translocation of FoxO1, thus inhibiting the transcriptional activity of the IDE promoter. Together, these findings imply a novel role of FADD in the reduction of protein stability and expression levels of IDE.

INTRODUCTION

Previous studies have reported that the Fas-FasL pathway and the downstream caspase-8 play important roles in islet mass and insulin secretion (Chinnaiyan et al., 1995). As a classical adaptor in Fas-FasL signaling, Fas-associated death domain-containing protein (FADD) also participates in a series of nonapoptotic processes regulated by its phosphorylation (Bonnet et al., 2011; Hua et al., 2003; Imtiyaz et al., 2009; Kabra et al., 2001; Lee et al., 2012; Matsuyoshi et al., 2006; Pyo et al., 2005; Shimada et al., 2006; Thomas et al., 2004; Welz et al., 2011; Yao et al., 2013; 2015). However, until now, its role in insulin degradation has not yet been evaluated.

It has been reported that overexpression of Fas in β cells leads to the formation of autoimmune diabetes (Moriwaki et al., 1999). In addition, Fas was also found to affect the production of insulin; insulin secretion is inhibited in Fas-deficient mice (Strandmark and Hallberg, 2007). These studies

proposed that the Fas signaling pathway might play important roles in insulin production and secretion. Previous studies performed in our lab showed that FADD-D mice, which mimic the constitutive phosphorylation of FADD, displayed an obviously decreased islet area (Yao et al., 2015). FADD phosphorylation was found to be involved in glucose metabolism, which resulted in low blood glucose, elevated insulin levels, decreased mRNA expression levels of insulin, and decreased glucose-stimulated insulin secretion (GSIS) in FADD-D mice. The islet secretion function of FADD-D mice was impaired probably due to developmental defects. Impaired insulin secretion and continuously elevated insulin levels in serum thus present us with the hypothesis that FADD-D mice might be associated with insulin degradation disorders (Yao et al., 2015).

The liver is the major tissue that helps remove approximately 50% of circulating insulin, which regulates liver glucose and lipid metabolism. Hepatic insulin clearance therefore contributes to regulating insulin action by controlling insulin availability to peripheral tissues (Bojsen-Moller et al., 2018). The underlying mechanism of hepatic metabolism by insulin is vital for understanding both normal physiology and the pathogenesis of metabolic diseases, such as hyperglycemia and hypertriglyceridemia (Rubenstein et al., 1972; Titchenell et al., 2017).

Insulin-degrading enzyme (IDE) is responsible for the degradation of a number of hormones and peptides, including insulin, and clears ~50% of insulin during the first portal passage (Duckworth et al., 1998; Villa-Perez et al., 2018). IDE knockout mice displayed a diabetic phenotype, exhibiting hyperinsulinemia and glucose intolerance (Abdul-Hay et al., 2011). IDE mutant mice were found to exhibit impaired GSIS as well as increased levels of insulin in pancreatic islets (Steneberg et al., 2013). In addition, human genetic studies have suggested that IDE polymorphisms are associated with the pathogenesis of diabetes mellitus (Bonnefond et al., 2010). Although it is well-known that IDE plays an important role in modulating blood glucose by insulin degradation, relatively little is known about the mechanisms of IDE regulation.

To the best of our knowledge, our investigations on IDE in livers of FADD-D mice reveal, for the first time, that FADD, especially in its phosphorylated form, has an impact on IDE regulation. We therefore have expanded the understanding of the non-apoptotic functions of FADD and its phosphorylation.

MATERIALS AND METHODS

Plasmids and reagents
The pEGFP-N1-FoxO1 plasmid and pEGFP-N1-TSS plasmid were kindly provided by Prof. D. Accili (Naomi Berrie Diabetes Center, Department of Medicine, College of Physicians & Surgeons of Columbia University, USA). The human IDE promoter (1-900) was cloned into the *SAC* I and *Hind* III restriction sites of the pGL3-basic vector (Promega, USA). The polymerase chain reaction (PCR) primer sequences used for plasmid construction were forward-CGAGCTCAAAGTAAC-CACTGAAGCCG and reverse-GGAAGCTTATTCCGCTTAC-CCACACAGG. Dulbecco's modified Eagle's medium (DMEM),

Opti-MEM, and Lipofectamine 2000 reagent were obtained from Invitrogen/Thermo Fisher Scientific (USA). Fetal bovine serum (FBS) was obtained from Sigma-Aldrich (USA). Anti-IDE, anti-GAPDH, anti-SIRT1, and anti-β-actin antibodies were from Santa Cruz Biotechnology (USA); anti-FADD and anti-CK-18 were from Abcam (USA); anti-FoxO1 was from Cell Signaling Technology (USA); and HRP goat-anti-mouse IgG, HRP rabbit-anti-goat IgG, and HRP goat-anti-rabbit IgG were purchased from Jackson ImmunoResearch Europe (USA). Alexa Fluor 488 donkey anti-rabbit IgG and goat anti-rabbit IgG were obtained from Invitrogen/Thermo Fisher Scientific. The immunohistochemical and DAB substrate kits were obtained from Shenzhen Fumax Technology (China). The SIRT1 inhibitor EX527 and activator SRT1720 were purchased from APExBIO (USA). DNase I was purchased from Sangon Biotech (China). Act D, collagenase IV, and DAPI were obtained from Sigma-Aldrich. All other chemicals were purchased from Sigma-Aldrich.

Animals
All studies involving mice were conducted in accordance with the high standards of animal welfare approved by the Nanjing University Animal Care and Use Committee in China (20180413). Animals were maintained in a specific pathogen-free animal facility on a 12-h light-dark cycle at an ambient temperature of 21°C. They were given free access to food and water. Detailed protocols for generating FADD-D mice have been described previously (Hua et al., 2003). Adult FADD-D and wild-type (WT) control mice of both sexes were used for the experiments.

Cell culture
HepG2, HEK293, and HEK293T cells were obtained from the Cell Bank of the Chinese Academy of Science (China). Cells were cultured in DMEM (Gibco/Thermo Fisher Scientific) supplemented with 10% FBS, 50 μg/ml streptomycin, and 50 U/ml penicillin. The primary hepatocytes were maintained in low-glucose DMEM supplemented with 20% FBS, 50 μg/ml streptomycin, and 50 U/ml penicillin. Cells were maintained at 37°C in a humidified incubator with 5% CO_2.

Primary hepatocytes extraction and cell culture
A 1.5% pentobarbital sodium solution was warmed in a water bath (37°C); thereafter, 5 min before perfusion, 100 μl of this solution was injected. The hepatic portal vein was exposed by carefully moving the viscera to the right of the abdominal cavity. Then, an 18-gauge angiocath was inserted into the hepatic portal vein. The perfusate tubing was connected to the needle, and infusion was initiated in situ at a low flow rate (10 ml/min) with 5 ml of prewarmed (37°C) D-hank's solution with 1,000 U heparin (Sigma-Aldrich). If performed properly, the liver would instantly begin to blanch. Once successful cannulation was confirmed, a cut was made at the inferior vena cava (IVC) to allow efflux. A further test for successful cannulation was performed by applying light pressure with a sterile swab on the IVC, leading to all lobes of the liver quickly beginning to swell. The flow rate of the infusion was increased to 25 ml/min. The liver became pale in color. The perfusion solution was replaced with 5 ml of

D-hank's solution plus collagenase IV (3 mg/ml) (Sigma-Aldrich) with no interruption in the flow for an additional 6 min. After collagenase perfusion, the liver began to appear spongy. The liver was resected and placed in a prechilled sterile beaker with 5 ml of DMEM and DNase I (1 mg/ml) (Sangon Biotech) and then moved to a tissue cell culture hood. Under the hood, a cell scraper was used to gently disperse the cells into DMEM in a sterile Petri dish. The cell dispersion was filtered through a 100 μm pore size cell strainer into a 50 ml conical tube in order to remove the connective tissues and undigested tissue fragments. The cells were then suspended in 40 ml of DMEM and centrifuged at 50g for 3 min at 4°C. The supernatant was aspirated, and the cells were gently resuspended in 40 ml of cold DMEM to wash the cells. Centrifugation was repeated, the supernatant was aspirated, and the cells were gently resuspended in 15 ml of DMEM. The cells were counted within the cell suspension using a hemocytometer, and cell viability was determined by trypan blue staining.

siRNAs and transfection

All synthetic siRNAs and negative controls (NCs) were purchased from GenePharma (China). Cells were transiently transfected with siRNAs or plasmids using Lipofectamine 2000 according to the manufacturer's instructions. The siRNA sequence of the target was as follows: FADD-5'-CACAGAGAAGGAGAACGCA-3'.

Luciferase reporter assay

For dual-luciferase reporter assays, HEK293T cells were seeded in a 24-well plate at a density of 1×10^5 cells per well in antibiotic-free medium one day prior to transfection. HEK293T cells were transfected with siRNA/NC and then cotransfected with IDE-promoter luciferase and control pCMV-RL reporter for 24 h. Each well of cells was transiently cotransfected with 0.8 μg of pGL-basic3-IDE plasmids, 0.8 μg of pEGFP-N1-FoxO1 plasmid or pEGFP-N1-TSS plasmid, and 8 ng of *Renilla* reporter plasmid (pCMV-RL; Promega) as an internal control using Lipofectamine 2000. The luciferase activity was measured consecutively using the Dual-Luciferase reporter assay (Promega).

RNA extraction and quantitative real-time PCR (RT-qPCR)

Total RNA was extracted from tissues and cells with TRIzol reagent (Invitrogen/Thermo Fisher Scientific) following the manufacturer's instructions. RT-qPCR was performed using a reverse transcription kit (Takara, Japan) and SYBR Green PCR Master Mix (Roche, Switzerland). RT-qPCR was performed on an ABI system (Applied Biosystems, USA). Primer sequences were as follows: IDE, 5'-GCCGCCGATCACAGCAGCAGGAG-3' and 5'-CCCACAGACCGGTAGCCCAGGAT-3'; FADD, 5'-GCCGCGCCTGGGGAAGAAGAC-3' and 5'-GCAAAGCAGCGGCCCATCAGGA-3'; β-actin, 5'-CATCGAGCACGGCATCGTCA-3' and 5'-TAGCACAGCCTGGATAGCAAC-3'. All data are represented as the means of the fold change from triplicate analyses and normalized to β-actin.

Western blotting (WB)

Liver samples were taken from the mice and snap-frozen in liquid N$_2$ and then stored for subsequent protein extractions. The tissue samples and cells were lysed in ice-cold lysis buffer for 30 min. The supernatant was boiled with Laemmli sample buffer for SDS-PAGE. Antibodies were sourced as follows: anti-FADD (1:500) (Abcam); anti-IDE (1:500), anti-SIRT1 (1:1,000), anti-β-actin (1:2,000), and anti-GAPDH (1:2,000) (Santa Cruz Biotechnology); HRP goat-anti-mouse IgG (1:3,000), HRP goat-anti-rabbit IgG (1:3,000), and HRP rabbit-anti-goat IgG (1:1,000) (Jackson ImmunoResearch Europe).

Histology

Livers obtained from the euthanized mice were fixed in 10% phosphate-buffered formalin and embedded in paraffin, and then 5-μm-thick sections were stained for routine histology. For immunohistochemical staining, the liver sections and primary hepatocytes were immunostained with anti-IDE antibody (1:300) (Santa Cruz Biotechnology) and visualized with DAB (Shenzhen Fumax Technology). From immunofluorescence staining, the expression levels of CK-18 and FoxO1 were detected. An immunofluorescence assay was used to detect the localization of cells with anti-FoxO1 antibody (1:1,000) (Cell Signaling Technology) and the identification of the primary hepatocyte cells with anti-CK-18 (1:1,000). Alexa Fluor 488-conjugated anti-rabbit IgG antibody and anti-mouse IgG antibody (1:1,000) (Invitrogen/Thermo Fisher Scientific) were used as secondary antibodies. Nucleic DNA was stained with 4,6-diamidino-2-phenylindole (DAPI) (Sigma-Aldrich). Images were then visualized with an Axiophot 2 microscope (Zeiss, Germany). Cells climbing to the carry sheet glass were stained according to the instructions of the PAS kit (Nanjing JianCheng Bioengineering Institute, China). Briefly, cell slides were washed with phosphate-buffered saline (PBS) three times. Primary hepatocytes were stained for 10 min for glycogen detection. After being rinsed under running water for 5 min, the cell slides were then stained for 10 s using the other reagent and then washed under running water again. The cell slides were sealed after drying. Periodic acid-Schiff (PAS)-positive glycogen was stained red or purple-red with blue nuclei. Images were then visualized with an Axiophot 2
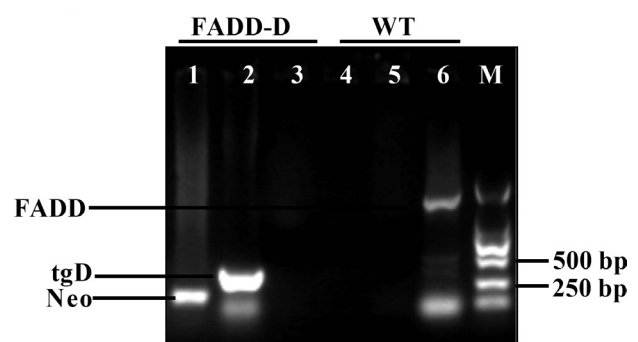

Fig. 1. Genotyping results for FADD-D and WT mice. Lanes 1-3: FADD-D mice. The FADD-TgD gene and FADD-Neo gene were amplified, and the FADD-Endo gene was not amplified. Lanes 4-6: WT mice. Only the FADD-Endo gene was amplified. M: marker 2000 bp.

microscope.

Statistical analysis

Data are presented as the mean ± SEM. Differences between two groups was analyzed by two-tailed Student's *t*-test using GraphPad Prism 6.0 (GraphPad Software, USA). Values were considered statistically significant at $P < 0.05$.

RESULTS

Genotyping of FADD-D mice

The construction of the mouse model was described in detail in our previously published paper (Hua et al., 2003). As shown in Fig. 1, the correct bands for the FADD-Neo gene

and TgD gene were amplified except for the FADD-Endo gene in FADD-D mice, while the correct bands for the FADD-Endo gene were amplified except for the FADD-Neo gene and the TgD gene in WT mice. The results indicated that the FADD-Endo gene had been knocked out completely, suggesting that FADD-D mice were the target mice for our subsequent study.

Identification of the primary hepatocytes

Primary hepatocytes needed to be used in the following experiments; thus, we first investigated whether the primary hepatocytes were extracted from the livers of living mice successfully. As shown in Fig. 2A, the cells displayed attachment and stretching, round, oval, polygonal, and dual-core phe-
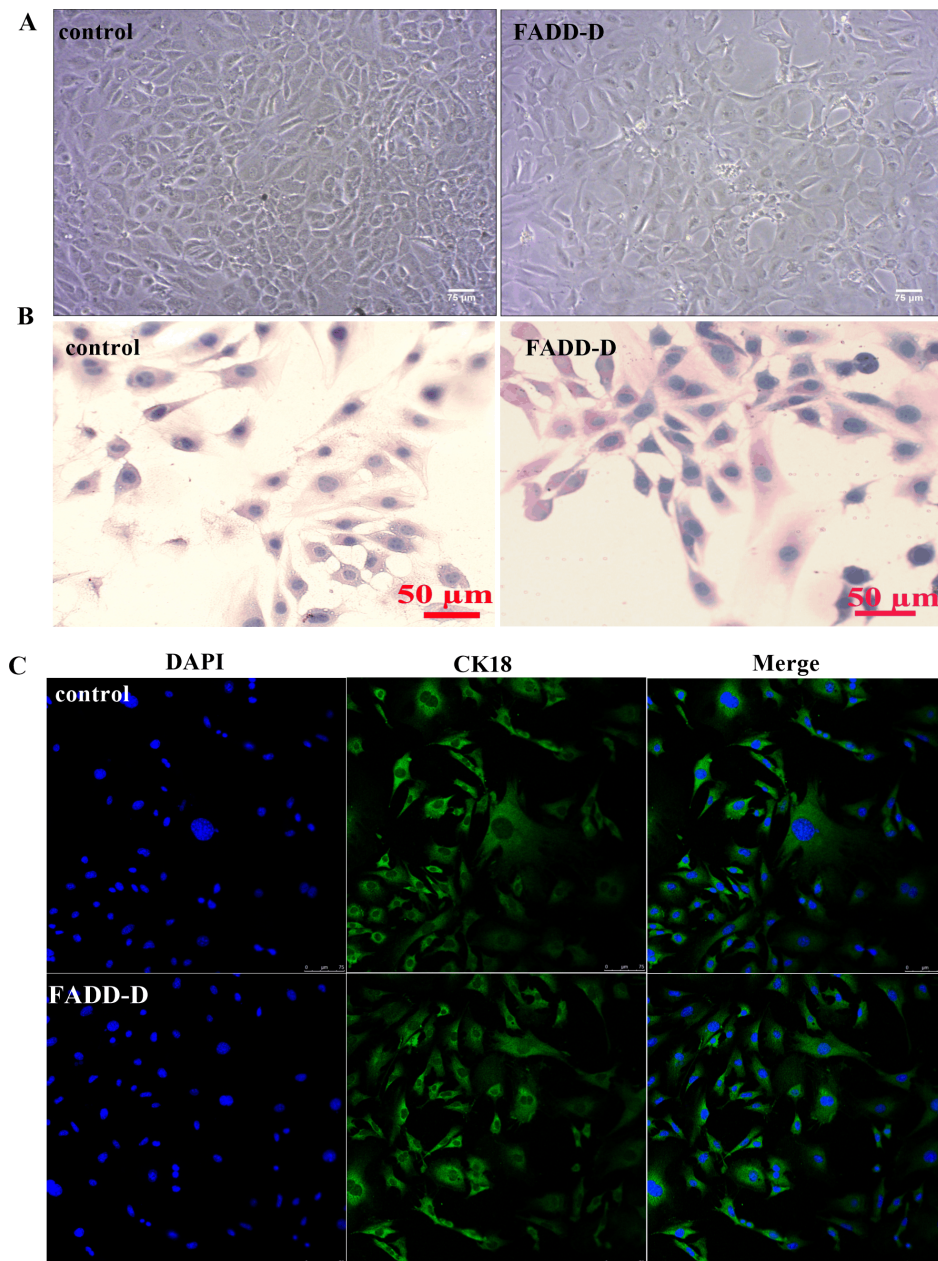

Fig. 2. Identification of the primary hepatocytes. (A) The morphology of the control and FADD-D primary hepatocytes. Scale bars = 75 μm. (B) PAS staining of primary hepatocytes extracted from the control and FADD-D mice. Scale bars = 50 μm. (C) CK-18 immunofluorescence assay for primary hepatocytes extracted from control and FADD-D mice. Scale bars = 75 μm.

notypes under the microscope. The cytoplasm was granular, and the cell boundary profile was clearly visible. PAS staining showed that the cytoplasm was stained by glycogen in the primary hepatocytes extracted from FADD-D mice and the control mice. Moreover, the amount of glycogen was found to be elevated in FADD-D mice compared with the control mice (Fig. 2B), which might be associated with the elevated serum insulin levels in FADD-D mice. Cytokeratin-18 (CK-18) is a normal component of the cytoskeleton of hepatocytes. Our immunofluorescence assay also showed that the hepatocytes were stained with green fluorescence by the CK-18

antibody (Fig. 2C).

Downregulation of IDE in the livers and primary hepatocytes from FADD-D mice

Previous studies performed in our lab showed that FADD-D mice exhibited increased insulin levels in serum and decreased insulin secretion (Yao et al., 2015). To explore the underlying mechanisms, the expression level of IDE was examined in the current study. Our data showed that both the mRNA and protein expression levels of IDE were downregulated in the liver (Figs. 3A and 3B) and primary hepatocytes (Figs. 3D and
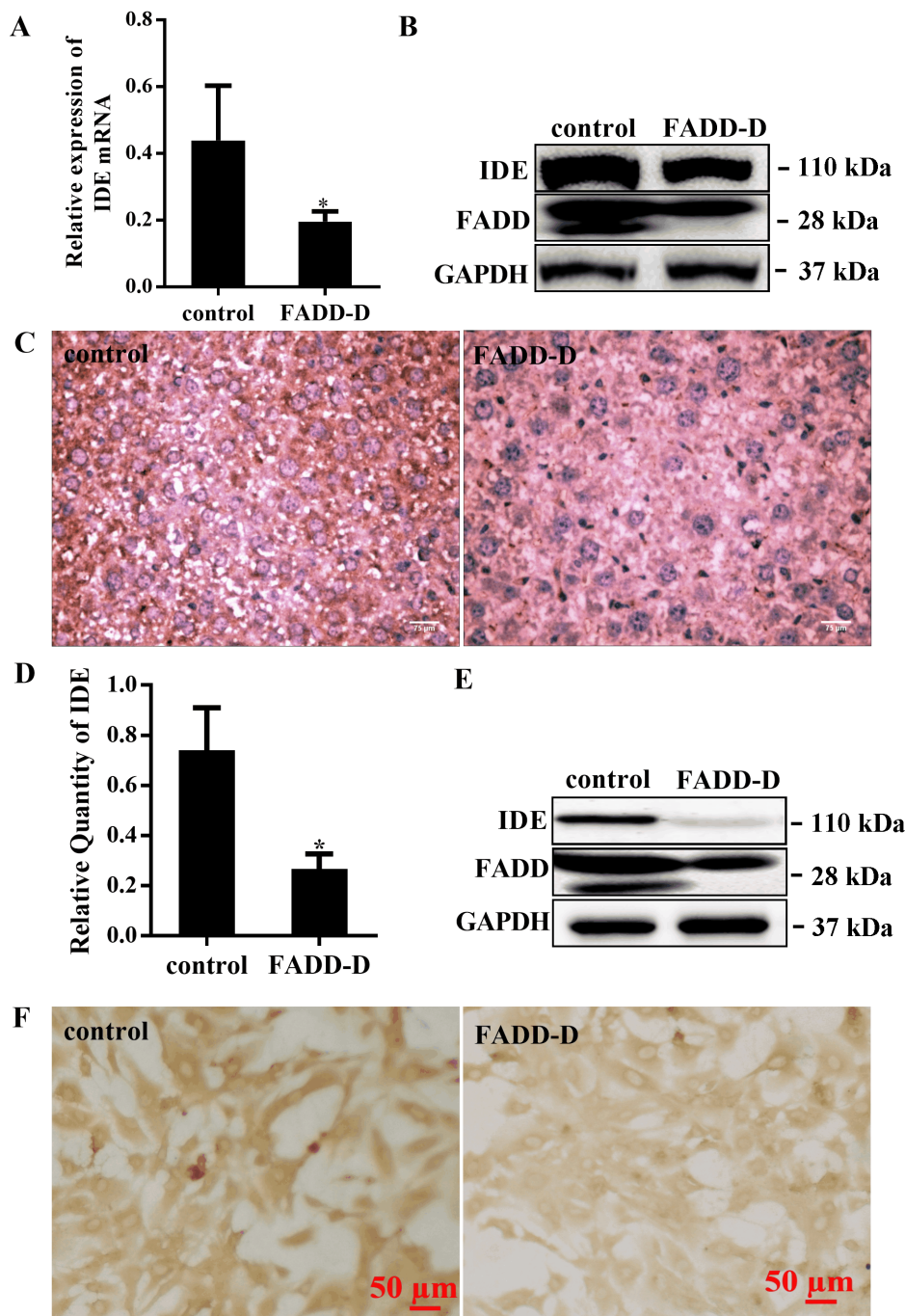

Fig. 3. Reduced mRNA and protein expression levels of IDE in FADD-D liver and primary hepatocytes. (A) The mRNA expression level of IDE in livers. (B) The protein expression level of IDE in livers. (C) The expression level of IDE in livers detected by immunohistochemistry analysis. Scale bars = 75 μm. (D) The mRNA expression level of IDE in primary hepatocytes. (E) The protein expression level of IDE in primary hepatocytes. (F) The expression level of IDE in primary hepatocytes detected by immunohistochemistry analysis. Scale bars = 50 μm. Data are represented as mean ± SD, $*P < 0.05$ compared with the respective control.

3E) in FADD-D mice by qPCR and WB analyses. Immunohistochemistry staining also confirmed that the protein level of IDE in FADD-D liver and primary hepatocytes was downregulated (Figs. 3C and 3F). In FADD-D mice, the expression level of IDE was reduced, while the concentration of serum insulin remained elevated (Yao et al., 2015). Thus, we speculate that the increased insulin level might be caused by less insulin degradation due to the reduced expression of IDE.

Reduced IDE expression in FADD-knockdown HepG2 cells

Our previous studies indicated that FADD deficiency sometimes displays similar effects or phenotypes to FADD phosphorylation (Cheng et al., 2014; Zhuang et al., 2016). Thus, to further investigate the effect of FADD on IDE, we next determined the stability of IDE mRNA in response to FADD knockdown in HepG2 cells. As shown in Figs. 4A and 4C, the expression level of FADD also decreased in cells transfected with FADD siRNA. We found that both the mRNA and protein levels of IDE were downregulated in HepG2 cells transfected with FADD siRNA fragments by qPCR and WB analyses (Figs. 4B and 4C). The mRNA level of IDE may be regulated by IDE transcription or the stability of mRNA. To further address this issue, 5 μg/ml actinomycin D (Act D) was added to HepG2 cells transfected with siFADD or NC fragments on a variable time gradient. The results showed that the stability of IDE mRNA did not change markedly after transfection with siFADD compared with the control (Fig. 4D). Thus, we concluded that FADD knockdown might affect the transcription of IDE but not the stability of IDE mRNA.

Effects of FADD phosphorylation or deficiency on IDE protein stability

To further assess the effect of FADD phosphorylation on IDE, we concentrated our subsequent analysis on IDE protein levels with cycloheximide (CHX) stimulation in primary hepatocytes from FADD-D and control mice. The results showed that the degradation rate of the IDE protein increased in cells from FADD-D mice compared to those from the control (Figs. 5A and 5B). Similarly, the degradation rate of IDE protein also increased in HEK293 cells transfected with siFADD stimulated with CHX for 24 h compared to those transfected with NC (Figs. 5C and 5D). In addition, we found that the expression levels of IDE decreased progressively following insulin stimulation at different concentrations in primary hepatocytes from FADD-D mice compared to the control (Fig. 5E). Together, these data suggested that FADD might be involved in the regulation of IDE protein stability.

FoxO1 inhibited the luciferase activity of the IDE promoter in FADD-D or FADD knockdown cells

Insulin activity in maintaining balanced glycolipid metabolism partly accounts for the phosphorylation of FoxO1 (Cheng and White, 2011). Phosphorylation of FoxO1 at Thr24, Ser256, and Ser319 (TSS) can promote its nuclear to cytoplasmic translocation and inhibit FoxO1-dependent transcription. We first aimed to explore the relationship between FoxO1 phosphorylation and the IDE promoter by luciferase activity analysis. We found that the transcription activity of the IDE promoter in HEK293T cells transfected with the pEGFP-N1-FoxO1 plasmid was the lowest, while HEK293T cells transfected with the pEGFP-N1 plasmid had the highest transcription activity (Fig. 6A), indicating that FoxO1 might be critical
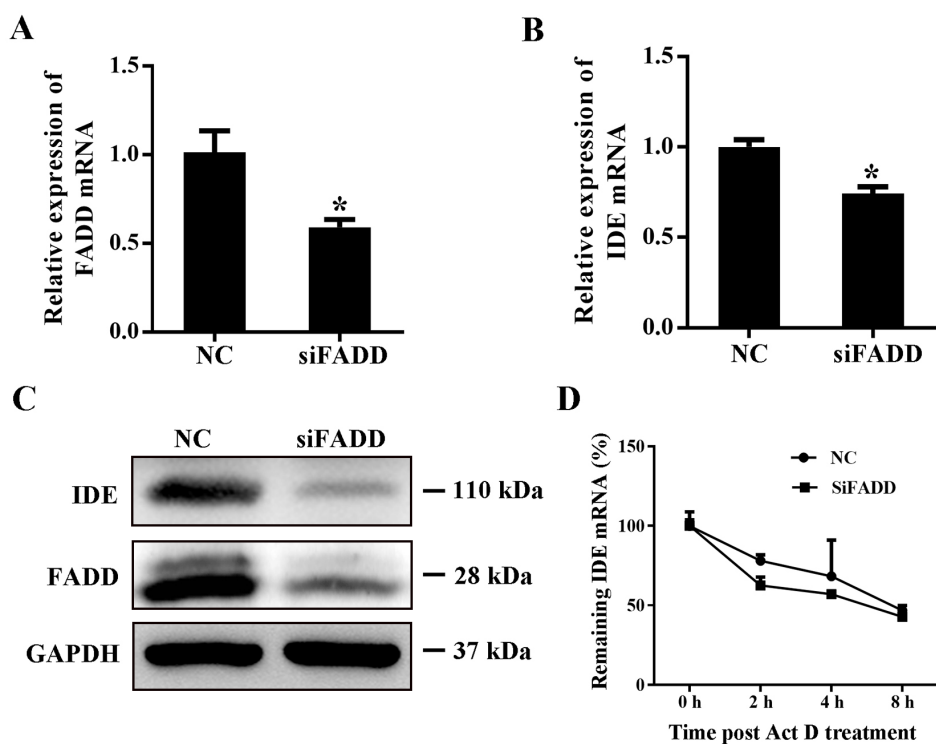

Fig. 4. Reduced IDE expression level in FADD-knockdown HepG2 cells. The mRNA levels of (A) FADD and (B) IDE and (C) the protein expression level of IDE in HepG2 cells transfected with FADD interference fragments. (D) HepG2 cells were transfected with the NC/siFADD fragment and then treated with 5 μg/ml Act D for 0, 2, 4, and 8 h to detect the degradation rate of IDE mRNA. Data are represented as mean ± SD, *$P < 0.05$ compared with the respective control.
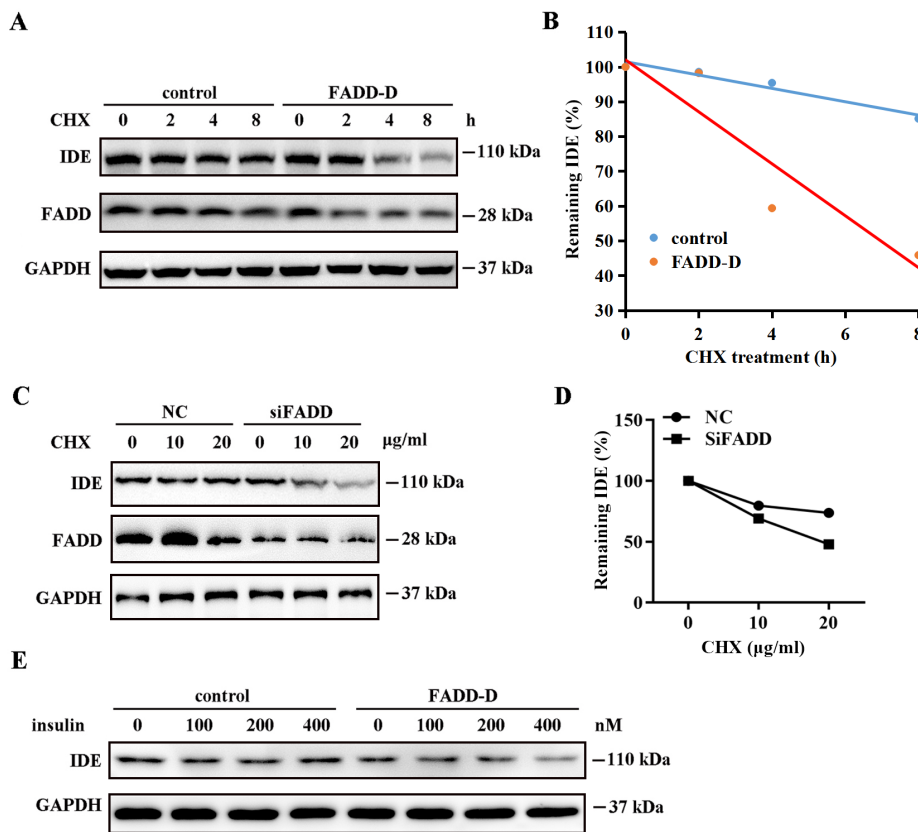
A

B

C

D

E

Fig. 5. The effect of FADD phosphorylation or knockdown on IDE protein stability. (A) Western blotting analysis of IDE in primary hepatocytes from control and FADD-D mice upon CHX (20 µg/ml) treatment for 0, 2, 4, and 8 h. (B) The rate of IDE degradation. (C) Western blotting analysis of IDE in HEK293T cells transfected with siFADD or NC in response to CHX treatment at the indicated concentrations for 24 h. (D) The rate of IDE degradation. (E) Primary hepatocytes extracted from control and FADD-D mice were treated with insulin at different concentrations (0, 100, 200, and 400 nM) for 12 h, and then the protein level of IDE was examined by WB analysis.

to block the transcription of the IDE promoter. Interestingly, cells transfected with pEGFP-N1-TSS exhibited higher transcription activity than those transfected with pEGFP-N1-FoxO1 (Fig. 6A). To further investigate the relationship between IDE and FADD, we next determined the transcriptional activity of the IDE promoter in response to FADD knockdown in HEK293T cells. As shown in Fig. 6B, by interfering with the expression of FADD in HEK293T cells, reduced luciferase activity was observed, indicating that the IDE transcription activity in HEK293T cells transfected with FADD siRNA fragments was decreased. In addition, by WB analysis, we found that the protein level of IDE was downregulated in HEK293T cells transfected with FADD siRNA fragments (Fig. 6C). To further observe the effect of FADD phosphorylation on the cellular localization of FoxO1, an immunofluorescence experiment was carried out on primary hepatocytes from FADD-D and control mice. The results showed that FADD phosphorylation promoted the movement of FoxO1 from the cytoplasm to the nucleus (Fig. 6D), suggesting that FADD phosphorylation might affect FoxO1 nuclear localization and subsequently decrease IDE transcription activity.

Effects of Sirt1 on IDE expression

It is well known that Sirt1 has a prominent role in the liver, where it can deacetylate FoxO1 proteins, resulting in a pronounced effect on glucose homeostasis and insulin secretion. Sirt1 deacetylates FoxO1 and enables the activation of FoxO1 transcription in multiple systems (Cao et al., 2016; Sin et al., 2015; Xiong et al., 2011). Here, in our study, to observe the

effect of Sirt1 on IDE expression, different concentrations of the Sirt1 inhibitor EX527 and activator SRT1720 were added to HepG2 cells. The results showed that Sirt1 negatively regulated the expression of IDE in HepG2 cells. We noticed that when Sirt1 was inhibited, the expression of IDE was upregulated; on the other hand, when Sirt1 was activated, the expression of IDE was downregulated (Fig. 7A). Furthermore, Sirt1 was found to be elevated in FADD-knockdown HepG2 cells (Fig. 7B). Based on these data, we therefore speculated that FADD might regulate the expression of IDE through the Sirt1-FoxO1 signaling pathway. However, the detailed regulatory mechanisms of FADD on Sirt1 still need to be investigated in our future research.

DISCUSSION

FADD is a critical adaptor in apoptosis signaling shared by several death receptors, and its phosphorylation mediates many nonapoptotic activities (Hua et al., 2003). In our previous research, we found that FADD phosphorylation plays an important role in islet morphology and function via proteomics discovery and further physiological validation. FADD-D mice displayed increased insulin levels in serum; however, the function of insulin secretion was impaired in FADD-D mice (Yao et al., 2015). Therefore, we speculate that elevated insulin levels in the serum of FADD-D mice might not be due to abnormal synthetic progress but may be related to abnormal degradation. To address this issue, we thus focused on insulin degradation in FADD-D mice. In this study, the
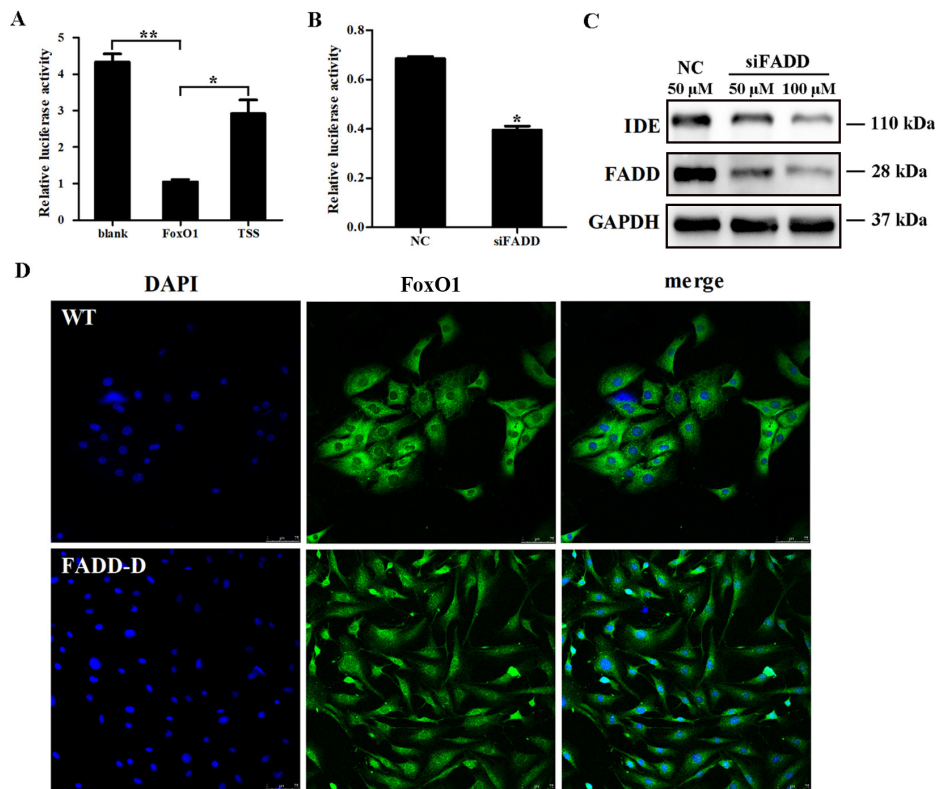
Fig. 6. FoxO1 inhibited the luciferase activity of the IDE promoter. (A) Plasmids (pEGFP-N1, pEGFP-N1-FoxO1, and pEGFP-N1-TSS) were transfected into HEK293T cells, and the luciferase activity of the IDE promoter was detected 24 h after transfection. Data are represented as the fold change of luciferase activity of the pGL3 basic vector. (B) HEK293T cells were transfected with siFADD or NC fragment, and then the luciferase activity of the IDE promoter was detected. (C) HEK293T cells were transfected with siFADD or NC fragment, and then the protein level of IDE was detected. (D) The immunofluorescence results of FoxO1 in primary hepatocytes extracted from control and FADD-D mice. FoxO1 (green), DAPI (blue) staining (3 mice per group); scale bars = 75 μm. Data are represented as mean ± SD. *$P < 0.05$, **$P < 0.01$ compared with the respective control.
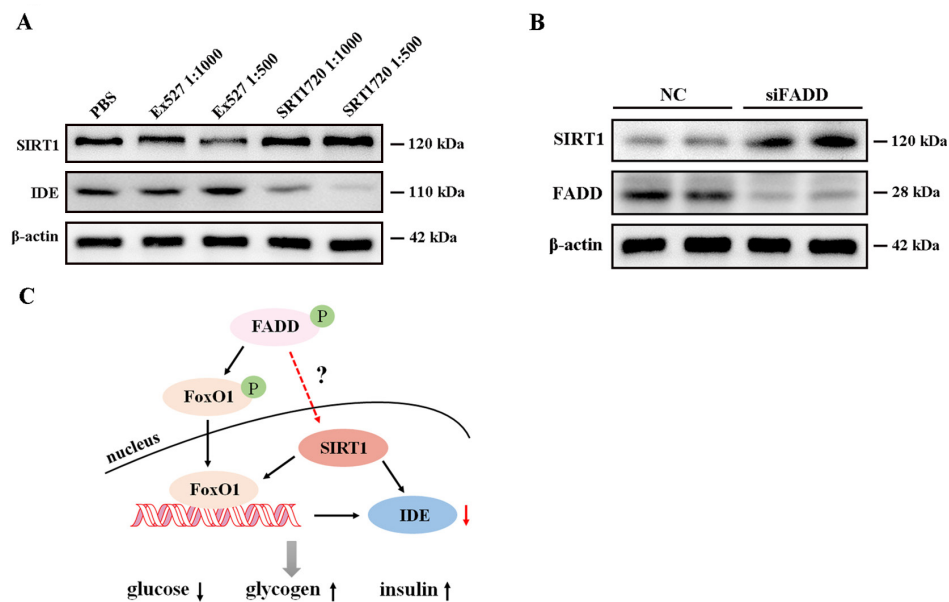

Fig. 7. Sirt1 regulates the expression level of IDE. (A) Western blotting analysis of IDE in HepG2 cells treated with PBS, Sirt1 inhibitor EX527 (1:1,000, 1:500) or activator Sirt1720 (1:1,000, 1:500). (B) The expression level of Sirt1 in HepG2 cells transfected with siFADD. (C) Schematic illustration of the potential mechanisms by which FADD affects the expression level of IDE.

FADD-D mouse model was used to study the effect of FADD phosphorylation on the expression of IDE for the first time, providing new insights into the function of FADD. FADD phosphorylation or downregulation might inhibit IDE stability and affect the nuclear location of FoxO1, leading to reduced IDE expression and the subsequent slowed degradation of insulin and decreased blood glucose.

IDE is an intracellular 110 kDa thiol zinc-metalloendopeptidase that is located in the cytosol, peroxisomes, endosomes, and on the cell surface. IDE catalyzes the degradation of several small proteins, such as insulin, amylin and β-amyloid (Shen et al., 2006). Genetic association studies in humans have proven that IDE plays an important role in the pathogenesis of T2DM (Pivovarova et al., 2015). Liver-specific deletion of IDE (L-IDE-KO) in mice resulted in elevated plasma glucose levels and reduced plasma membrane insulin receptor levels in the liver (Villa-Perez et al., 2018). Once the function of IDE is impaired, the biological effects and degradation of insulin will be abnormal, thus leading to hyperinsulinemia (Rezende et al., 2014). Valid and selective modulators of IDE activity can be potential drugs for T2DM treatment (Pivovarova et al., 2016). Vettorazzi et al. (2017) used taurine conjugated bile acid (TUDCA) which can stimulate the expression of IDE in HepG2 cells to ameliorate hyperinsulinemia induced by obesity.

IDE is the principal enzyme in the insulin degradation process in the liver (Pivovarova et al., 2015; Valera Mora et al., 2003). We hypothesized that FADD phosphorylation may have an effect on the expression of IDE in the liver. Our data showed that the mRNA and protein levels of IDE were significantly decreased in FADD-D mouse hepatic tissue and the same results were also obtained in the liver primary hepatocyte cells. After the primary hepatocytes cells were stimulated by varying exposure times of CHX and varying concentrations of insulin, the protein level of IDE reduced gradually in FADD-D primary hepatocytes, but did not change significantly in control cells. Similar results were also found in HEK293 cells transfected with FADD siRNA. Together, these results indicated that FADD phosphorylation or FADD downregulation could affect the protein stability of IDE.

FoxO1 was shown to play a major role in regulating the insulin response in the liver, which is one of its critical sites of action. When FoxO1 constitutively expresses in the liver, fasting blood glucose rises (Matsumoto et al., 2006). Conversely, liver specific FoxO1 knockout mice develop fasting hypoglycemia (Matsumoto et al., 2007). FoxO1 is active in the fasted state and distributed in the nucleus, which results in the transcriptional induction of two gluconeogenic enzymes and increased hepatic glucose production (Zhang et al., 2006). In the fed state, phosphorylation of three highly conserved protein kinase B sites, corresponding to TSS in human FoxO1, suppresses transactivation and promotes nuclear exclusion of FoxO1 proteins (Lu et al., 2012). In our study, we found that FoxO1 negatively regulated on IDE promoter activity. In FADD-D primary hepatocytes, more FoxO1 moved from the cytoplasm into the nucleus, indicating that FADD phosphorylation affected the nuclear localization of FoxO1. Due to the negative regulation of FoxO1, the expression of IDE was then downregulated with subsequent suppression of gluconeo-genesis and hyperinsulinemia.

Previous studies have shown that FADD is an adaptor in the Fas-FasL apoptosis signaling pathway, which takes part in the development of autoimmune diabetes by β cells (Silva et al., 2003). In addition, since FADD is located on chromosome 11q13.3, a diabetes susceptibility locus, it has been suspected that changes in FADD might be a possible contributor to type 1 diabetes (Pirot et al., 2008). Subsequent studies revealed that FADD is located outside of the type 1 diabetes mellitus region on chromosome 11q13 (IDDM4); thus it is unlikely to be the gene for IDDM4 (Eckenrode et al., 2000). Zhang et al. (2013) identified an upstream promoter element that blocks the reverse transcription of the mouse IDE promoter through promoter deletion and mutation analysis. Although there are a few reports showing that FADD is related to glucose, the specific mechanism is not yet clear. In the present study, FADD phosphorylation may reduce the expression of IDE by promoting the nuclear translocation of FoxO1. In addition, Sirt1 might also take part in regulating the expression of IDE, which then affects insulin degradation, the growth of glycogen, and the decrease in blood glucose (Fig. 7C).

Our study preliminarily explored the impact of FADD phosphorylation on IDE. However, further studies are needed; for instance, determination of the binding site of FoxO1 on the IDE promoter and how Sirt1 is involved in the regulation of insulin degradation. When HepG2 cells were treated with a Sirt1 inhibitor and activator, Sirt1 negatively regulated the expression of IDE. The detailed regulatory mechanism of FADD on Sirt1 requires further experimental confirmation.

In summary, our investigations revealed for the first time that FADD, especially in its phosphorylated form, has an impact on IDE expression. FADD phosphorylation or downregulation reduces the expression of IDE by inhibiting its transcription by promoting the translocation of FoxO1 into the nucleus and decreasing IDE protein stability. We have thereby expanded the understanding of the nonapoptotic functions of FADD and its phosphorylation. These findings implied a novel role of FADD in the reduction of protein stability and expression levels of IDE.

AUTHOR CONTRIBUTIONS
Z.C.H. and H.Z. designed the outline of the paper and secured funding. Y.L. and H.Z. wrote the manuscript. Y.L. performed most experiments in this study and prepared the figures. J.L., C.Y., and Y.Y. performed the experiments with the animals. J.C. and J.W. helped with the western blotting experiments. H.Z. and Y.L. analyzed data. All authors have read and approved the final version of this manuscript.

CONFLICT OF INTEREST

The authors have no potential conflicts of interest to disclose.

ORCID

Yan Lin	https://orcid.org/0000-0002-8051-3409
Jia Liu	https://orcid.org/0000-0001-6053-7692
Jia Chen	https://orcid.org/0000-0003-0301-4494
Chun Yao	https://orcid.org/0000-0002-7228-3252
Yunwen Yang	https://orcid.org/0000-0002-5435-3624
Jie Wang	https://orcid.org/0000-0002-9725-6023
Hongqin Zhuang	https://orcid.org/0000-0001-6183-711X
Zi-Chun Hua	https://orcid.org/0000-0002-3740-1639

REFERENCES

Abdul-Hay, S.O., Kang, D., McBride, M., Li, L., Zhao, J., and Leissring, M.A. (2011). Deletion of insulin-degrading enzyme elicits antipodal, age-dependent effects on glucose and insulin tolerance. PLoS One 6, e20818.

Bojsen-Moller, K.N., Lundsgaard, A.M., Madsbad, S., Kiens, B., and Holst, J.J. (2018). Hepatic insulin clearance in regulation of systemic insulin concentrations-role of carbohydrate and energy availability. Diabetes 67, 2129-2136.

Bonnefond, A., Froguel, P., and Vaxillaire, M. (2010). The emerging genetics of type 2 diabetes. Trends Mol. Med. 16, 407-416.

Bonnet, M.C., Preukschat, D., Welz, P.S., van Loo, G., Ermolaeva, M.A., Bloch, W., Haase, I., and Pasparakis, M. (2011). The adaptor protein FADD protects epidermal keratinocytes from necroptosis in vivo and prevents skin inflammation. Immunity 35, 572-582.

Cao, Y., Jiang, X., Ma, H., Wang, Y., Xue, P., and Liu, Y. (2016). SIRT1 and insulin resistance. J. Diabetes Complications 30, 178-183.

Cheng, W., Zhang, R., Yao, C., He, L., Jia, K., Yang, B., Du, P., Zhuang, H., Chen, J., Liu, Z., et al. (2014). A critical role of Fas-associated protein with death domain phosphorylation in intracellular reactive oxygen species homeostasis and aging. Antioxid. Redox Signal. 21, 33-45.

Cheng, Z. and White, M.F. (2011). Targeting Forkhead box O1 from the concept to metabolic diseases: lessons from mouse models. Antioxid. Redox Signal. 14, 649-661.

Chinnaiyan, A.M., O'Rourke, K., Tewari, M., and Dixit, V.M. (1995). FADD, a novel death domain-containing protein, interacts with the death domain of Fas and initiates apoptosis. Cell 81, 505-512.

Duckworth, W.C., Bennett, R.G., and Hamel, F.G. (1998). Insulin degradation: progress and potential. Endocr. Rev. 19, 608-624.

Eckenrode, S., Marron, M.P., Nicholls, R., Yang, M.C., Yang, J.J., Guida Fonseca, L.C., and She, J.X. (2000). Fine-mapping of the type 1 diabetes locus (IDDM4) on chromosome 11q and evaluation of two candidate genes (FADD and GALN) by affected sibpair and linkage-disequilibrium analyses. Hum. Genet. 106, 14-18.

Hua, Z.C., Sohn, S.J., Kang, C., Cado, D., and Winoto, A. (2003). A function of Fas-associated death domain protein in cell cycle progression localized to a single amino acid at its C-terminal region. Immunity 18, 513-521.

Imtiyaz, H.Z., Zhou, X., Zhang, H., Chen, D., Hu, T., and Zhang, J. (2009). The death domain of FADD is essential for embryogenesis, lymphocyte development, and proliferation. J. Biol. Chem. 284, 9917-9926.

Kabra, N.H., Kang, C., Hsing, L.C., Zhang, J., and Winoto, A. (2001). T cell-specific FADD-deficient mice: FADD is required for early T cell development. Proc. Natl. Acad. Sci. U. S. A. 98, 6307-6312.

Lee, E.W., Seo, J., Jeong, M., Lee, S., and Song, J. (2012). The roles of FADD in extrinsic apoptosis and necroptosis. BMB Rep. 45, 496-508.

Lu, M., Wan, M., Leavens, K.F., Chu, Q., Monks, B.R., Fernandez, S., Ahima, R.S., Ueki, K., Kahn, C.R., and Birnbaum, M.J. (2012). Insulin regulates liver metabolism in vivo in the absence of hepatic Akt and Foxo1. Nat. Med. 18, 388-395.

Matsumoto, M., Han, S., Kitamura, T., and Accili, D. (2006). Dual role of transcription factor FoxO1 in controlling hepatic insulin sensitivity and lipid metabolism. J. Clin. Invest. 116, 2464-2472.

Matsumoto, M., Pocai, A., Rossetti, L., Depinho, R.A., and Accili, D. (2007). Impaired regulation of hepatic glucose production in mice lacking the forkhead transcription factor Foxo1 in liver. Cell Metab. 6, 208-216.

Matsuyoshi, S., Shimada, K., Nakamura, M., Ishida, E., and Konishi, N. (2006). FADD phosphorylation is critical for cell cycle regulation in breast cancer cells. Br. J. Cancer 94, 532-539.

Moriwaki, M., Itoh, N., Miyagawa, J., Yamamoto, K., Imagawa, A., Yamagata, K., Iwahashi, H., Nakajima, H., Namba, M., Nagata, S., et al. (1999). Fas and Fas ligand expression in inflamed islets in pancreas sections of patients with recent-onset type I diabetes mellitus. Diabetologia 42, 1332-1340.

Pirot, P., Cardozo, A.K., and Eizirik, D.L. (2008). Mediators and mechanisms of pancreatic beta-cell death in type 1 diabetes. Arq. Bras. Endocrinol. Metabol. 52, 156-165.

Pivovarova, O., Hohn, A., Grune, T., Pfeiffer, A.F., and Rudovich, N. (2016). Insulin-degrading enzyme: new therapeutic target for diabetes and Alzheimer's disease? Ann. Med. 48, 614-624.

Pivovarova, O., von Loeffelholz, C., Ilkavets, I., Sticht, C., Zhuk, S., Murahovschi, V., Lukowski, S., Docke, S., Kriebel, J., de las Heras Gala, T., et al. (2015). Modulation of insulin degrading enzyme activity and liver cell proliferation. Cell Cycle 14, 2293-2300.

Pyo, J.O., Jang, M.H., Kwon, Y.K., Lee, H.J., Jun, J.I., Woo, H.N., Cho, D.H., Choi, B., Lee, H., Kim, J.H., et al. (2005). Essential roles of Atg5 and FADD in autophagic cell death: dissection of autophagic cell death into vacuole formation and cell death. J. Biol. Chem. 280, 20722-20729.

Rezende, L.F., Camargo, R.L., Branco, R.C., Cappelli, A.P., Boschero, A.C., and Carneiro, E.M. (2014). Reduced insulin clearance and lower insulin-degrading enzyme expression in the liver might contribute to the thrifty phenotype of protein-restricted mice. Br. J. Nutr. 112, 900-907.

Rubenstein, A.H., Pottenger, L.A., Mako, M., Getz, G.S., and Steiner, D.F. (1972). The metabolism of proinsulin and insulin by the liver. J. Clin. Invest. 51, 912-921.

Shen, Y., Joachimiak, A., Rosner, M.R., and Tang, W.J. (2006). Structures of human insulin-degrading enzyme reveal a new substrate recognition mechanism. Nature 443, 870-874.

Shimada, K., Nakamura, M., Ishida, E., and Konishi, N. (2006). Molecular roles of MAP kinases and FADD phosphorylation in prostate cancer. Histol. Histopathol. 21, 415-422.

Silva, D.G., Petrovsky, N., Socha, L., Slattery, R., Gatenby, P., and Charlton, B. (2003). Mechanisms of accelerated immune-mediated diabetes resulting from islet beta cell expression of a Fas ligand transgene. J. Immunol. 170, 4996-5002.

Sin, T.K., Yung, B.Y., and Siu, P.M. (2015). Modulation of SIRT1-Foxo1 signaling axis by resveratrol: implications in skeletal muscle aging and insulin resistance. Cell. Physiol. Biochem. 35, 541-552.

Steneberg, P., Bernardo, L., Edfalk, S., Lundberg, L., Backlund, F., Ostenson, C.G., and Edlund, H. (2013). The type 2 diabetes-associated gene ide is required for insulin secretion and suppression of alpha-synuclein levels in beta-cells. Diabetes 62, 2004-2014.

Strandmark, K.M. and Hallberg, L.R.M. (2007). The origin of workplace bullying: experiences from the perspective of bully victims in the public service sector. J. Nurs. Manag. 15, 332-341.

Thomas, L.R., Henson, A., Reed, J.C., Salsbury, F.R., and Thorburn, A. (2004). Direct binding of Fas-associated death domain (FADD) to the tumor necrosis factor-related apoptosis-inducing ligand receptor DR5 is regulated by the death effector domain of FADD. J. Biol. Chem. 279, 32780-32785.

Titchenell, P.M., Lazar, M.A., and Birnbaum, M.J. (2017). Unraveling the regulation of hepatic metabolism by insulin. Trends Endocrinol. Metab. *28*, 497-505.

Valera Mora, M.E., Scarfone, A., Calvani, M., Greco, A.V., and Mingrone, G. (2003). Insulin clearance in obesity. J. Am. Coll. Nutr. *22*, 487-493.

Vettorazzi, J.F., Kurauti, M.A., Soares, G.M., Borck, P.C., Ferreira, S.M., Branco, R.C.S., Michelone, L.S.L., Boschero, A.C., Junior, J.M.C., and Carneiro, E.M. (2017). Bile acid TUDCA improves insulin clearance by increasing the expression of insulin-degrading enzyme in the liver of obese mice. Sci. Rep. *7*, 14876.

Villa-Perez, P., Merino, B., Fernandez-Diaz, C.M., Cidad, P., Lobaton, C.D., Moreno, A., Muturi, H.T., Ghadieh, H.E., Najjar, S.M., Leissring, M.A., et al. (2018). Liver-specific ablation of insulin-degrading enzyme causes hepatic insulin resistance and glucose intolerance, without affecting insulin clearance in mice. Metabolism *88*, 1-11.

Welz, P.S., Wullaert, A., Vlantis, K., Kondylis, V., Fernandez-Majada, V., Ermolaeva, M., Kirsch, P., Sterner-Kock, A., van Loo, G., and Pasparakis, M. (2011). FADD prevents RIP3-mediated epithelial cell necrosis and chronic intestinal inflammation. Nature *477*, 330-334.

Xiong, S., Salazar, G., Patrushev, N., and Alexander, R.W. (2011). FoxO1 mediates an autofeedback loop regulating SIRT1 expression. J. Biol. Chem. *286*, 5289-5299.

Yao, C., Zhuang, H., Cheng, W., Lin, Y., Du, P., Yang, B., Huang, X., Chen, S., Hu, Q., and Hua, Z.C. (2015). FADD phosphorylation impaired islet morphology and function. J. Cell. Physiol. *230*, 1448-1456.

Yao, C., Zhuang, H., Du, P., Cheng, W., Yang, B., Guan, S., Hu, Y., Zhu, D., Christine, M., Shi, L., et al. (2013). Role of Fas-associated death domain-containing protein (FADD) phosphorylation in regulating glucose homeostasis: from proteomic discovery to physiological validation. Mol. Cell. Proteomics *12*, 2689-2700.

Zhang, L., Ding, Q., Wang, P., and Wang, Z. (2013). An upstream promoter element blocks the reverse transcription of the mouse insulin-degrading enzyme gene. Biochem. Biophys. Res. Commun. *430*, 26-31.

Zhang, W., Patil, S., Chauhan, B., Guo, S., Powell, D.R., Le, J., Klotsas, A., Matika, R., Xiao, X., Franks, R., et al. (2006). FoxO1 regulates multiple metabolic pathways in the liver: effects on gluconeogenic, glycolytic, and lipogenic gene expression. J. Biol. Chem. *281*, 10105-10117.

Zhuang, H., Wang, X., Zha, D., Gan, Z., Cai, F., Du, P., Yang, Y., Yang, B., Zhang, X., Yao, C., et al. (2016). FADD is a key regulator of lipid metabolism. EMBO Mol. Med. *8*, 895-918.